forests

MDPI

Article

Rill Erosion Due to Wildfire or Deforestation in Forestlands of Northern Iran

Misagh Parhizkar [1,2], Manuel Esteban Lucas-Borja [3] and Demetrio Antonio Zema [2,*]

[1] Faculty of Agricultural Sciences, University of Guilan, Rasht 41996-13776, Iran; misagh.parhizkar@unirc.it
[2] Agraria Department, Mediterranean University of Reggio Calabria, Loc. Feo di Vito, I-89122 Reggio Calabria, Italy
[3] Department of Agroforestry Technology and Science and Genetics, School of Advanced Agricultural and Forestry Engineering, Campus Universitario, Castilla La Mancha University, E-02071 Albacete, Spain; ManuelEsteban.Lucas@uclm.es
* Correspondence: dzema@unirc.it

Abstract: Rill erosion, mostly affecting steep and long hillslopes, is one of the most severe effects of deforestation and wildfires in natural ecosystems. Specific monitoring and accurate but simple models are needed to assess the impacts of these forest disturbances on the rill detachment process. To address this need, this study has simulated the rill detachment capacity (D_c) through flume experiments on samples of soils collected in hillslopes after deforestation and severe burning. The associations between D_c and organic matter (OM) and the aggregate stability of soil (WSA), two key parameters influencing the rill detachment process, have also been explored under the two soil conditions (deforested and burned soils) using multivariate statistical techniques. Finally, linear regression models to predict D_c from these soil parameters or the hydraulic and morphological variables (water flow rate, WFR, and soil slope, S), set in the flume experiments, have been proposed for both soil conditions. Higher D_c in samples from deforested sites compared to the burned soils (+35%) was measured. This D_c increase was associated with parallel decreases in OM (−15%) and WSA (−34%) after deforestation compared to the wildfire-affected sites. However, the discrimination in those soil properties between the two soil conditions was not sharp. Accurate linear equations ($r^2 > 0.76$) interpolating D_c and the shear stress (τ) have been set to estimate the rill erodibility (K_r) to evaluate soil resistance in erosion models to be applied in deforested or burned sites.

Keywords: forest ecosystems; soil organic matter; soil aggregate stability; rill detachment capacity; shear stress; rill erodibility

Citation: Parhizkar, M.; Lucas-Borja, M.E.; Zema, D.A. Rill Erosion Due to Wildfire or Deforestation in Forestlands of Northern Iran. *Forests* **2024**, *15*, 1926. https://doi.org/10.3390/f15111926

Academic Editor: Carlos R. Mello

Received: 5 October 2024
Revised: 27 October 2024
Accepted: 28 October 2024
Published: 31 October 2024

1. Introduction

Anthropogenic activities in forests can alter the ecosystem characteristics, leading to noticeable changes in soil properties and erodibility [1,2]. Deforestation and wildfires are among the most severe factors of ecological degradation in forests [3,4], and greatly impact soil erosion [5,6]. The resulting damage to the geomorphological and ecological quality of forest ecosystems is an alarming threat to the future of the environment and humankind, and attention to these threats has been becoming nowadays more and more crucial [7,8]. In particular, soil erosion in forest environments has received careful attention in recent years from both the monitoring and modelling perspectives [9]. Much research has been carried out on the most important drivers of soil degradation in forest ecosystems [10], and both deforestation and wildfires have been recognised as key anthropogenic factors of soil erosion [11].

It is well known that deforestation and wildfire remove vegetation and leave the soil bare [12,13]. Furthermore, soil heating due to fire noticeably alters some key soil properties (e.g., water infiltration capacity, hydrophobicity level, and content of organic matter)

[14,15]. The decrease in ground cover and severe changes in its properties noticeably increase runoff generation and soil detachment in both deforested and fire-affected hillslopes [16,17], which inevitably leads to a huge production of sediments in valley areas [18]. On forest hillslopes with steeper profiles, soil erosion is mainly due to the formation of rills by the overland flow [19,20]. In this regard, "rill detachment capacity" (D_c) is defined [21,22] as the maximum value of soil detachment in rills of clear water (that is without any sediment load). Moreover, the so-called "rill erodibility" (K_r), that is, the increase in detachment rate for each additional unit of shear stress in rills, and "critical shear stress" (τ_c), that is, the soil's resistance to mobilization and the initiation of motion of soil particles, quantify the soil's ability to resist particle detachment caused by concentrated flows [23,24]. Therefore, K_r and τ_c are two key parameters to estimate the overall erosion using physically based prediction models [25,26]. Several past studies have demonstrated that D_c, K_r, and τ_c show a high variability according to changes in land use [27,28] and in key properties of soil, such as the organic matter content and stability of aggregates [29,30]. Therefore, physically based erosion models may give unrealistic predictions when essential input parameters, such as D_c, K_r, and τ_c, are affected by noticeable errors [31,32], especially if soil disturbance factors (e.g., deforestation, wildfires, management operations) increase the natural variability of those parameters [33,34].

Noticeable reductions in soil aggregate stability and organic matter are among the immediate impacts of wildfires and deforestation on forest ecosystems. For instance, refs. [35,36] stated that fire and deforestation remarkably reduce soil organic matter in pine forests of Spain, and in loess-derived soils in Iran, respectively. Overall, the literature is almost unanimous in associating the changes in these two important soil properties due to deforestation and fire with the alteration of runoff and erosion rates in forestlands.

In recent years, deforestation and wildfire have been significantly increasing trends in most countries, and this inevitably leads to increasing erosion rates [37–39]. Moreover, the impacts of deforestation and fire on soil's hydrological response will be exacerbated under the forecasted scenarios of climate change [40,41].

Many studies have explored the effects of wildfire and deforestation on rill erosion (e.g., [36,42,43]). However, the relevant investigations have been separately carried out in deforested (e.g., [43,44]) or severely burned (e.g., [45]) areas. No comparisons in D_c and key physical–chemical properties of disturbed soils (such as the organic matter content and aggregate stability) in forest ecosystems have been made, to the authors' best knowledge. The evaluation of the dynamics of organic matter and aggregate stability and their association with the rill detachment process in deforested and burned sites is essential to support land managers and public authorities, who must protect the forest ecosystems against natural and anthropogenic degradation [46–48].

To fill this gap and address this need, this study has modelled the changes in D_c due to wildfire and deforestation by flume experiments on soil samples collected in steep hillslopes of Northern Iran. The specific objectives are the following: (1) assessing the changes in soil organic matter, aggregate stability, and D_c in burned and deforested soils; and (2) analysing the possible discrimination in those properties between the two soil conditions using multivariate statistical techniques.

2. Materials and Methods

2.1. Study Area Experimental Site

The study area was the Khortum Forestland Park (coordinates 37°07′11″ N; 49°29′31″ E), covering an area of 70 hectares 17 km south of Rasht City (Northern Iran) at an altitude of 66 m above the mean sea level (Figure 1). The climate of the area is Mediterranean, Csa type, according to the Köppen classification system [49]. The mean temperature and rainfall are 16.3 °C and 1360 mm/year, respectively, according to historical weather data of the Iranian Meteorological Organization. The prevalent slope of the area is in the range of 3 to 39%. The soil texture is prevalently silty clay loam (sand 12.9%, silt 47.8%, and clay

39.3%), based on the findings of ref. [50], and can be classified as Cutanic Luvisols (Clayic) (WRB classification) and Ultic Hapludalfs (USDA classification). This park is one of the most visited destinations in Guilan Province, due to its children's playgrounds, bike and car paths, hiking trails, and rest areas on hillslopes. However, in recent years (10–12), unsustainable management has been practised in this park, such as deforestation by logging to install high-voltage towers, which was stopped one to three years before the investigation [19]. From then, the tourist density on holiday days and the number and frequency of cars on the soil increased. Moreover, forest fires with variable severity (from low, due to tourist barbecues, to high, for fraudulent fires) occurred in the park. These disturbances have caused noticeable impacts on the ecosystem, such as loss of biodiversity and severe changes in soil properties (e.g., compaction, ash leaching, and modifications in organic matter and nutrients).

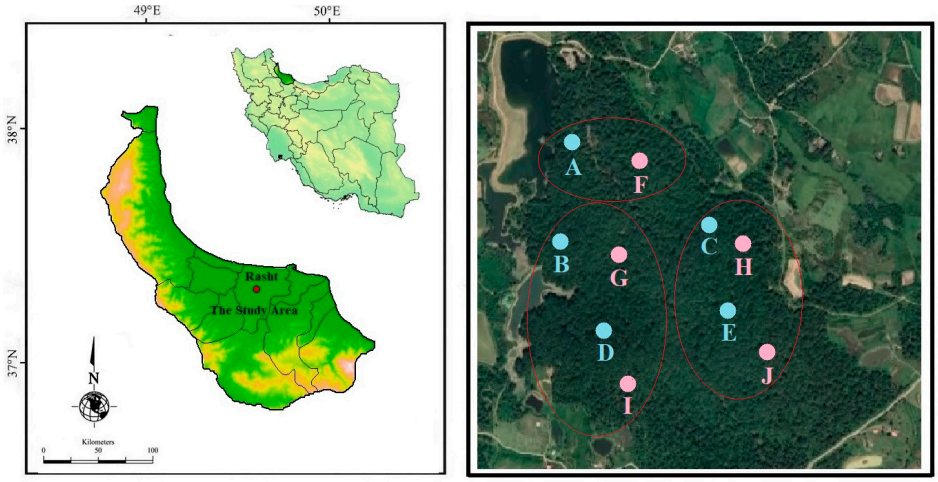

Figure 1. Geographical location of the study area (**left**) and an aerial view of the experimental sites (A to E, burned forestlands, and F to J, deforested lands) (**right**) in the study area (Khortum Forestland Park, Northern Iran) (source: Google® Map®).

2.2. Experimental Design

Ten experimental sites, of which five were burned by wildfires (hereinafter indicated as "B") and five deforested ("D"), were selected in the study area (Figure 1). The site characteristics were selected to be as homogenous as possible according to slope, type, texture, and past management of soils. Concerning the B sites, the fires were classified as being of low severity [51,52], based on the flame length (1.8–2.3 m) [53]. In the D sites, the vegetation cover was completely removed in the past to install high-voltage towers, and therefore the deforestation was severe [43].

The very similar characteristics (climate, soil, and vegetation) of the experimental sites, coupled with the same hydraulic conditions in the laboratory flume used for D_c modelling, allow a clear identification of changes in two key soil properties (soil organic matter and aggregate stability) and the rill detachment process for the case study.

2.3. Soil Sampling

Five soil samples, each of about 150–200 g, were collected in September 2022 from the soil surface (0–10 cm) in five experimental sites under each soil condition (B and D sites), totalling 50 samples (2 conditions × 5 sites × 5 samples). Since the operation was carefully and gently carried out, no variations in soil structure were detected. Soil samples were also collected in undisturbed (non-deforested and unburned) sites in a parent study [52]. The sampling depth was chosen to measure only rill erosion rates at the surface slope as influenced by the aforementioned factors (fire and deforestation) on the upper layer of soil.

After removing rocks, weeds, and litter, a steel ring with a diameter of 0.1 m and a height of 0.05 m was used to gently extract the sample from the ground. After collection, each soil sample was immediately transported to the laboratory, and the residual gravel and vegetation were removed by sieving (4 mm mesh) for the subsequent flume experiments until March 2023. Figure 2 reports the weather variability in the monitoring period (2022–2023).

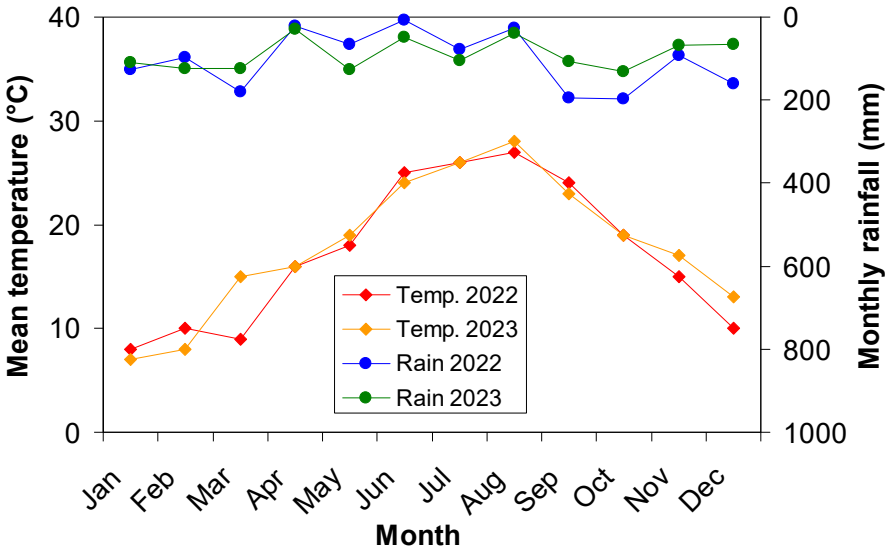

Figure 2. Variability in mean monthly temperature and rainfall in study area throughout the monitoring period (2022–2023) (Khortum Forestland Park, Northern Iran) (source: IRIMO).

2.4. Description of the Laboratory Flume and Experiments

The soil detachment process was simulated on the collected samples (area of 19.6 cm^2) in an experimental flume (width of 0.2 m, length of 3.5 m, and sides of 0.05 m) with a rectangular cross section (Figure 3). A 5 cm soil layer with a mean grain size of 5 mm (to be considered as non-erodible, the particles being coarse and the flow being shallow) was put over the flume bed, in order to reproduce the natural roughness of the soil [54]. The D_c was measured at five water flow rates (0.31, 0.42, 0.55, 0.67, and 0.79 L s^{-1}) and five soil slopes (4.2%, 10.2%, 16.1%, 24.4%, and 33.6%). These values were chosen according to the prevalent hydromorphological characteristics of the area, based on field measurements of overland flows and hillslope profiles in previous studies carried out in forestlands of the province [52,55]. Before each experiment (each repeated seven times under the same soil condition and slope, and water flow rate), the collected soil sample was saturated (28–30% *w*/*w*, equal to the field capacity, and bulk density of about 1490 kg/m^3) by absorption by placing its bottom in a water container for 24 h [56]. Then, the sample was covered with a panel, to prevent scouring due to the water flow adjustments. The sample was placed in a hole with the same dimensions as the steel ring on the downward side of the flume. The ring was positioned with its central axis aligned with the longitudinal axis of the flume (and then with the water surface). The soil slope of the flume bed was first set at the desired value by adjusting the profile of the flume. Then, tap water was poured from upstream, and the stabilised water flow rate was measured five times per experiment by collecting water in a graduated plastic cylinder for a given time. After removing the panel on the sample, the experiment started with soil scouring. Each run ended when the depth of the eroded soil in the steel ring reached approximately 0.015 m—measured at a graduated scale inside the ring—or after five minutes [20,57], in order to minimize the influence of the side-wall of the steel ring on the D_c. The steel ring was not taken out after each experiment under a specific soil slope and water discharge. However, this does not affect

the detachment process at a scouring depth over 15 mm [48]. After the experiment ended, the soil in the sampler was oven-dried at 105 °C for 24 h and then weighed.

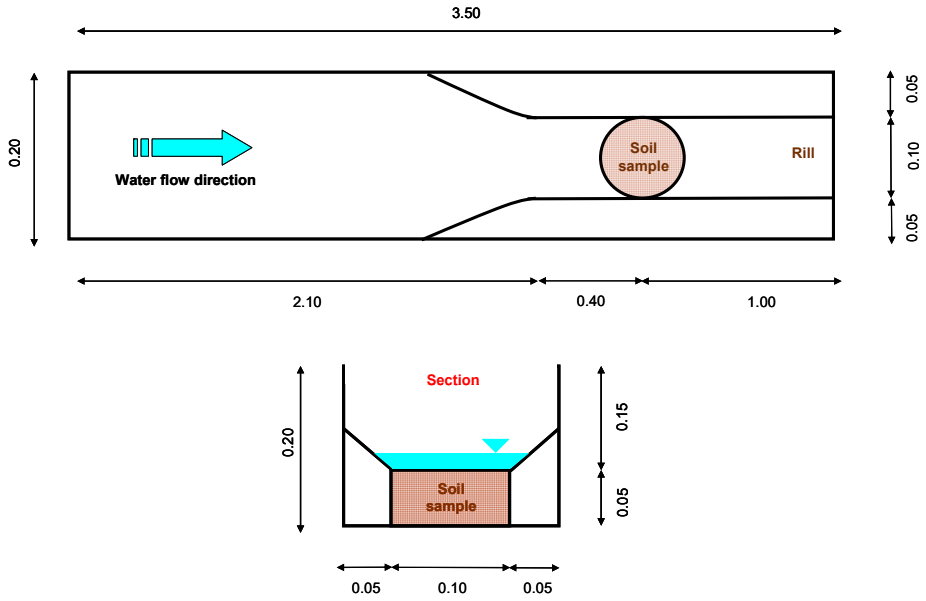

Figure 3. Laboratory flume (plant and section) used to simulate rill detachment on soil samples collected in the study area (Khortum Forestland Park, Northern Iran).

The experimental design consisted of two soil conditions (B and D sites) × five soil slopes × five water flow rates × seven replications per experiment, totalling 350 experiments with as many measures of D_c.

2.5. Measurement of Hydraulic Parameters and Rill Detachment Capacity

With stabilised water in the flume, the flow depth (h, [m]) was measured using a level-probe with an accuracy of 1 mm and averaged across three points in each of two cross sections (0.4 m, over the scouring point, and 1 m upstream of the flume outlet, in an undisturbed place): in the centre of the flume, and at 0.01 m from each side. The flow conditions were variable along the experimental flume, mainly due to the water turbulence and viscosity as well as the presence of the water inlet and outlet, and this made the flow depths and, as a consequence, the mean velocity (V, calculated as the ratio between the water flow and depth) variable point by point. However, the flow condition was uniform in the area, where the sample was positioned, and the water viscosity influenced only the water regime (expressed by Reynolds number). Since flow velocity is a key parameter to estimate the hydraulic variables associated with the soil detachment process, following the methodology suggested by [58], the value of surface velocity (V_s, [m s^{-1}]) was directly measured over the soil sample in five replications using a fluorescent dye technique [59,60]. The Reynolds number (Re, [–]) was calculated from the values of V_s and h (also measured over the sample) to identify the flow regime, which was laminar under each flow condition (Re < 1200). A reduction coefficient of 0.6 (extracted among the values of 0.6, 0.7, or 0.8 for laminar, transitional, or turbulent flow, respectively, suggested by ref. [61], was applied to V_s to calculate V in the scouring section. The water temperature (T, [°C]) was also recorded to calculate the water viscosity (approx. 10^{-6} m^2 s^{-1}).

Based on the measured hydraulic parameters over the scouring point (Table 1), the flow shear stress (τ, [Pa]) [25] was calculated using the following equation:

$$\tau = \rho g R S \quad (1)$$

where ϱ is the clean water density [kg m^{-3}], g is the acceleration of gravity [m s^{-2}], R is the hydraulic radius [m], and S is the slope of the flume bed [m m^{-1}].

Table 1. Hydraulic parameters to calculate D_c after the flume experiments on soil samples of burned and deforested sites in the study area (Khortum Forestland Park, Northern Iran).

Experiment (Each with 7 Replications)	Slope [S, %]	Flow Discharge [Q, L s^{-1}]	Flow Depth [h, mm]	Flow Velocity [V, m s^{-1}]	Hydraulic Radius [R, mm]	Flow Velocity [V_s, m s^{-1}] *	Shear Stress [τ, Pa]
1	4.2	0.062	4.1	0.38	3.94	0.27	1.62
2		0.084	5.5	0.38	5.21	0.35	2.15
3		0.110	6.8	0.40	6.37	0.48	2.62
4		0.134	7.5	0.45	6.98	0.56	2.87
5		0.158	9.3	0.42	8.51	0.58	3.50
6	10.2	0.062	3.8	0.41	3.66	0.38	3.66
7		0.084	5.1	0.41	4.85	0.46	4.85
8		0.110	6.3	0.44	5.93	0.58	5.92
9		0.134	7.1	0.47	6.63	0.67	6.63
10		0.158	8.4	0.47	7.75	0.77	7.75
11	16.1	0.062	3.4	0.46	3.29	0.41	5.19
12		0.084	4.3	0.49	4.12	0.49	6.50
13		0.110	5.2	0.53	4.94	0.59	7.80
14		0.134	6.1	0.55	5.75	0.67	9.07
15		0.158	7.3	0.54	6.80	0.79	10.73
16	24.4	0.062	2.3	0.67	2.25	0.53	5.38
17		0.084	2.8	0.75	2.72	0.62	6.51
18		0.110	3.6	0.76	3.47	0.71	8.31
19		0.134	4.7	0.71	4.49	0.78	10.73
20		0.158	5.9	0.67	5.57	0.86	13.32
21	33.6	0.062	2.1	0.74	2.06	0.61	6.77
22		0.084	2.6	0.81	2.53	0.72	8.34
23		0.110	3.3	0.83	3.19	0.79	10.52
24		0.134	3.6	0.93	3.47	0.86	11.44
25		0.158	4.7	0.84	4.49	0.97	14.78

Note: * measured by the dye technique.

The rill detachment capacity (D_c, [kg s^{-1} m^{-2}] was calculated using the dry weight of detached soil (ΔM, [kg]) measured before and after the experiment, scouring time (Δt, [s]), and the area of the soil sample (A, [m^2]), as shown in Equation (2):

$$D_c = \frac{\Delta M}{A \cdot \Delta t} \quad (2)$$

2.6. Measurement of Soil Properties

Among the large number of soil properties that are impacted by human disturbance in forest soils, we specifically focused on organic matter (OM), and aggregate stability of soil. The latter are among the most sensitive properties to fire [14,15], and, moreover, it is well known that heavy machinery can severely modify soil structure, impacting OM stock and breaking soil aggregates [62,63]. To compare the changes in soil properties between B and D sites, organic matter content and aggregate stability in water (WSA) were measured on an additional 50 soil samples (5 samples × 5 sites × 2 soil conditions, each of 250 g) collected very close (less than 20–30 cm) to the points, where the samples for the flume experiments were extracted. These two soil properties, showing high variability after deforestation [64] and wildfire [65], were determined by the potassium dichromate colourimetric method [66] and the wet-sieving method [67], respectively, after sieving (4 mm mesh).

2.7. Modelling the Rill Detachment Capacity

After calculating the rill detachment capacity, rill erodibility (K_r, [s m^{-1}]) and critical shear stress (τ_c, [Pa]) were estimated as the slope and the intercept on the "y" axis, respectively, of the line interpolating D_c and shear stress, as shown in Equation (3) [68]:

$$D_c = K_r(\tau - \tau_c) \quad (3)$$

2.8. Statistical Analysis

A one-way ANOVA was used to identify significant differences in the soil properties and rill detachment capacity between the two soil conditions (burned and deforested soils) at p-level < 0.05. Previously, the normality of sample distribution was checked using QQ-plots.

Then, Pearson's correlation matrix was computed, to find associations (expressed by the coefficient of correlation, r) between pairs of soil parameters. A Principal Component Analysis (PCA) was also applied to explore whether one derivative variable (a Principal Component, PC) [69] can synthesise the original parameters, losing as little information as possible. The number of PCs explaining at least a percentage of 75% of the original variance was retained. The observations were grouped in clusters using Agglomerative Hierarchical Cluster Analysis (AHCA), a distribution-free ordination technique to group samples with similar characteristics by considering an original group of variables. As a similarity–dissimilarity measure, the Euclidean distance was used.

Finally, by coupling these multivariate statistical techniques (PCA and AHCA), the possible discrimination in D_c, WSA, and OM between B and D soils was assessed.

All statistical analyses were performed using XLSTAT software (Addinsoft, Paris, France, release 2019.1).

3. Results

3.1. Variations in Soil Properties and Rill Detachment Capacity Between Burned and Deforested Soils

According to the ANOVA, OM and WSA were significantly different between the burned (B) and deforested (D) sites ($F < 19.763$, $p < 0.001$) (Table 2). In more detail, both properties were significantly lower in D sites (1.06 ± 0.14%, OM, and 0.19 ± 0.05 mm, WSA)

compared to B areas (1.21 ± 0.1% and 0.25 ± 0.05 mm, respectively). Moreover, D_c was significantly (F = 5.320, $p < 0.05$) higher in D sites (0.06 ± 0.05 kg m^{-2} s^{-1}) compared to B areas (0.09 ± 0.05 kg m^{-2} s^{-1}) (Figure 4 and Table A1).

Table 2. Results of ANOVA applied to parameters measured on soil samples collected in burned and deforested sites in the study area (Khortum Forestland Park, Northern Iran).

Soil Parameters	Sum of Squares	Mean Squares	F	Pr > F
D_c	0.013	0.013	5.320	**0.025**
OM	0.307	0.307	21.862	**<0.0001**
WSA	0.050	0.050	19.763	**<0.0001**

Notes: D_c = rill detachment capacity; OM = soil organic matter; WSA = soil aggregate stability in water. Values in bold are significant at $p < 0.05$.

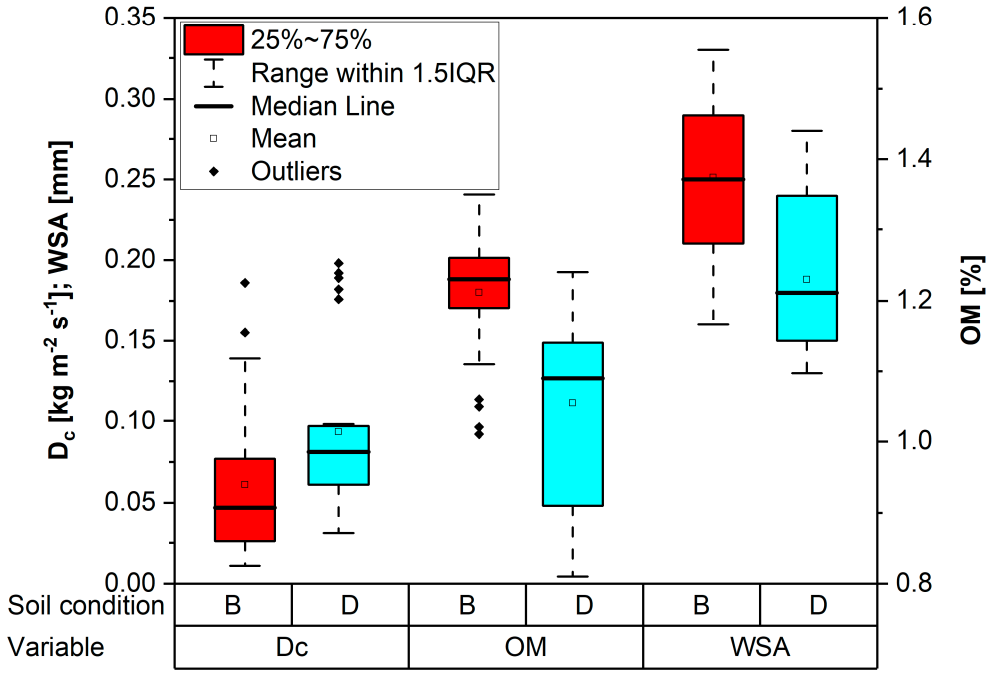

Figure 4. Boxplots of parameters measured in soil samples collected in burned and deforested sites ($n = 25$) of the study area (Khortum Forestland Park, Northern Iran); all differences between means were significant after Tukey's test ($p < 0.05$).

As expected, D_c increased under both soil conditions with water flow rate and soil slope. This increase was gradual at the lower soil slopes (4.2% to 16.1%). In contrast, a sudden increase in D_c was noticed at the highest flow rates for slopes higher than 24.4% (Figure 5 and Table A1).

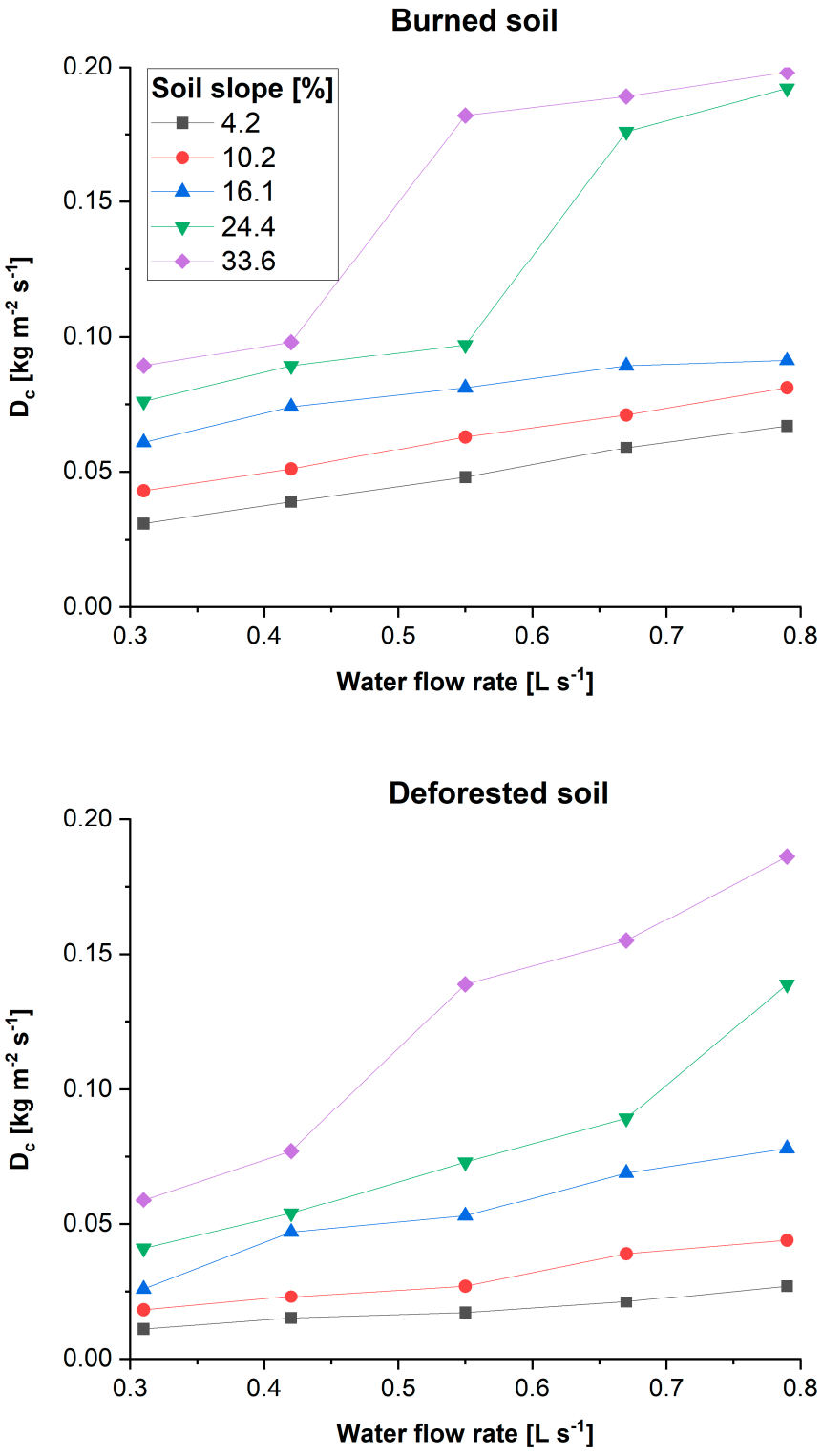

Figure 5. Variability in rill detachment capacity of according to the soil slope and water flow rate measured in flume experiments on soil samples collected in burned and deforested sites (Khortum Forestland Park, Northern Iran).

3.2. Analysis of Correlations Between Soil Parameters and Discrimination Between Burned and Deforested Soils

According to Pearson's correlations, high and negative coefficients between D_c on one side, and OM (r = −0.813) and WSA (r = −0.689) on the other side, were achieved, and these coefficients were always significant ($p < 0.001$). The latter parameters were also fairly and positively correlated with each other (r = 0.509) (Figure 6).

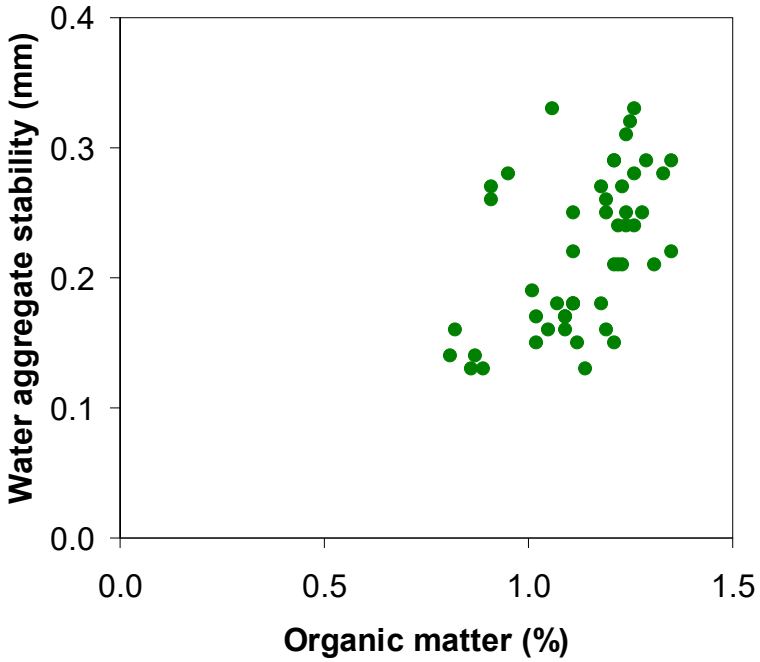

Figure 6. Correlation between organic matter content and water aggregate stability measured in soil samples collected in burned and deforested sites (Khortum Forestland Park, Northern Iran).

The PCA provided one derivative variable (the first PC), which alone explains 78.3% of the total variance in the original soil parameters, while the second PC explains only 16.8% of this variance. All parameters, which lay very close to the "x" axis, have very high loadings on the PC1, positive (0.950) for D_c, and negative for OM (−0.882) and for WSA (−0.818) (Figure 7). In other words, D_c is strongly linked to the latter soil properties, but it decreases when both OM and WSA increase.

PCA coupled with AHCA discriminated two separate clusters for the individual soil conditions. However, this discrimination was not sharp, since some observations overlap in the PC1 vs. PC2 scatterplot. In other words, the two clusters identified by AHCA did not include all soil samples collected in sites with homogenous conditions (deforested or burned). More specifically, the first cluster consisted of 20 B and 6 D samples, respectively, while the other cluster grouped 19 D and 5 B samples of soil (Figure 7). Therefore, the modelling activity was separately carried out for B and D soils.

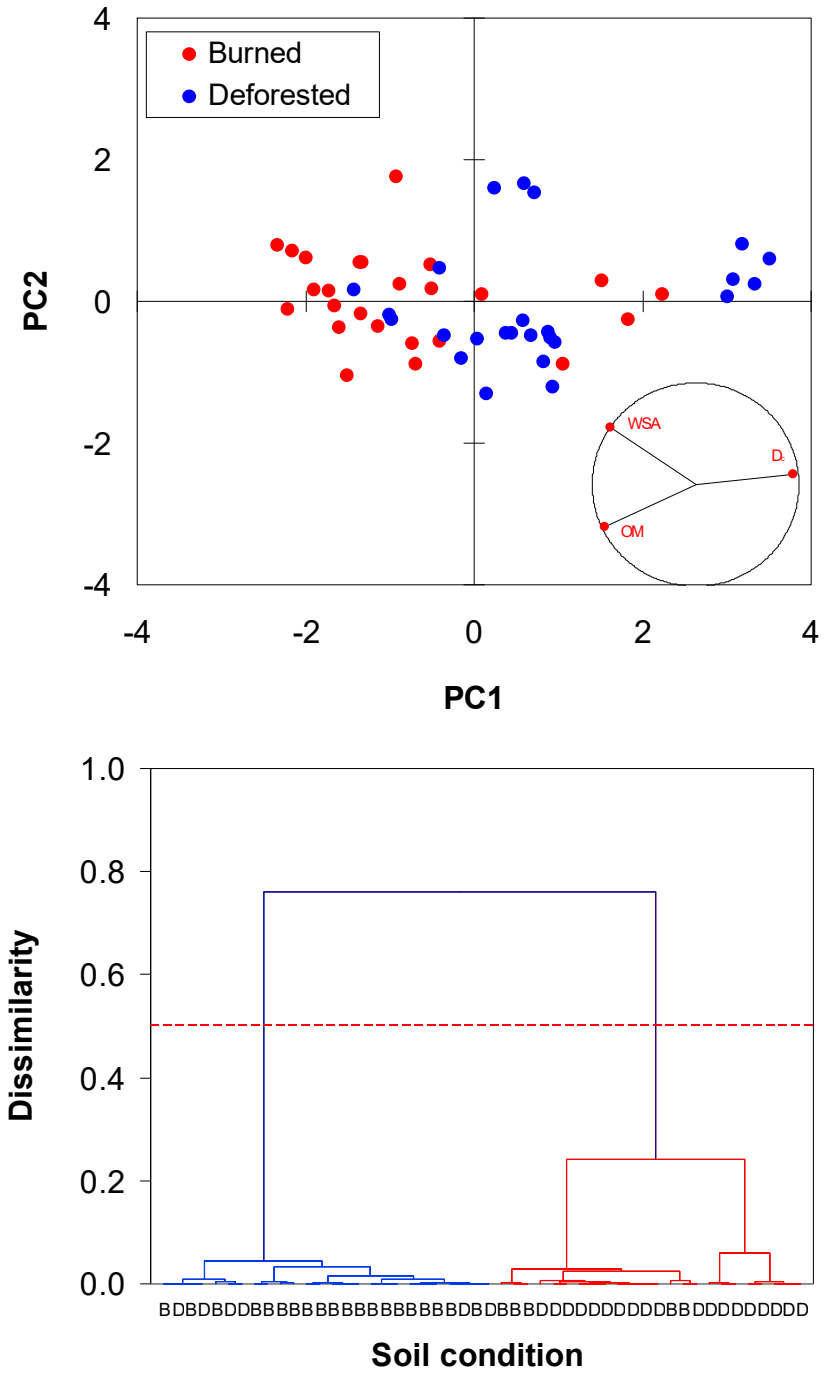

Figure 7. Biplot of soil properties (rill detachment capacity, D_c, soil organic matter, OM, and soil aggregate stability in water, WSA) (upper) and dendrogram (lower) provided by the Principal Component Analysis and Agglomerative Hierarchical Cluster Analysis, respectively, applied to soil samples collected in burned (B) and deforested (D) sites (n = 25) of the study area (Khortum Forestland Park, Northern Iran). Note: the lines in different colours highlight different clusters.

3.3. Modelling Rill Detachment Capacity in Burned and Deforested Soils

The linear interpolation of D_c and shear stress (τ) provided the values of the rill erodibility (K_r) for B and D sites with appreciable accuracy (coefficients of determination over 0.79, $p < 0.01$). The values of $K_{r\,c}$ were 0.0132 s m^{-1} in deforested sites and 0.0094 s m^{-1} in burned conditions (Figure 8). The intercept of the interpolating line was assumed to be

zero, in order to avoid negative and thus unrealistic values. Therefore, the critical value of τ (τ_c) should be considered null.

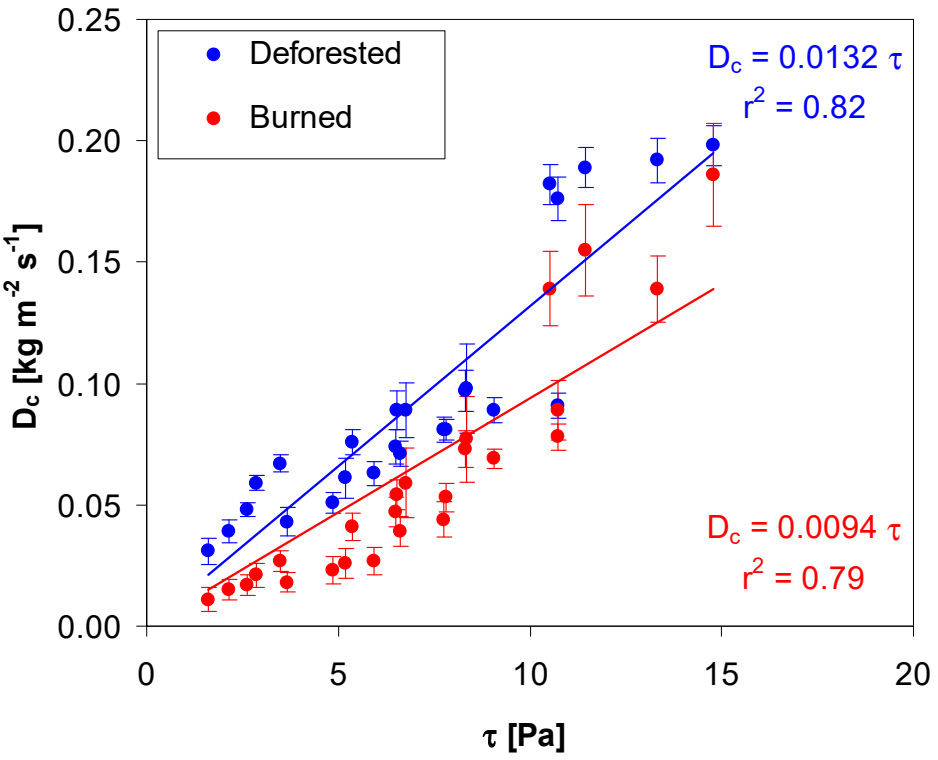

Figure 8. Linear interpolation between rill detachment capacity (D_c) and shear stress (τ) estimated by flume experiments on soil samples collected in burned and deforested sites of the study area (Khortum Forestland Park, Northern Iran). Vertical bars are the standard errors from the replicated measured of D_c in the flume experiments.

4. Discussion

4.1. Variations in Soil Properties and Rill Detachment Capacity Between Burned and Deforested Soils

Deforestation and wildfires are recognised worldwide as the most severe threats to forest ecosystems [70]. This study has evidenced that two key soil properties are noticeably impacted by these forest disturbances, but to different extents. Under these experimental conditions, deforestation reduces both soil properties by 15% for OM and 34% for WSA compared to the burned soils. A previous investigation, carried out by [52] in the same environment, measured a mean OM content of 1.74% and a WSA of 0.69 in undisturbed forests, which can be considered a natural and ideal condition. When these values are compared to the corresponding measurements of this study, it is evident that wildfire reduces OM by 30% and WSA by 64%, and the effects of deforestation are even more severe (reductions in OM and WSA by 39% and 73%, respectively).

These results may be surprising at first sight: both disturbances indeed remove the vegetal cover of the forest, but, in addition, soil heating due to fire further changes these important soil properties [71,72]. A deeper analysis of the measured data must consider two factors that may have influenced the soil response to fire and deforestation. First, the severity of the fire was low, which could have limited the detrimental effects that more severe wildfires exert on soil properties, such as the reduction in OM and destruction of soil aggregates [14,15]. Presumably, the soil temperature should not have been so high to result in almost total combustion of OM [73,74]. According to Varela et al. (2010), soil aggregate stability is not altered or slightly increases at temperatures up to 220 °C, and

therefore, such soil burning is not as severe as in the case of wildfires with long duration and high temperatures that noticeably impact soil aggregate stability [75,76]. The effects of forest fires on WSA can be more complex than other soil properties, such as organic matter content, microbiology, water repellency, and mineralogy [65], and this impact depends on many characteristics of soil and fire. Second, the site was deforested using heavy machinery, and this technique resulted in soil compaction that markedly reduced the WSA.

The higher OM content of the soil in the burned site in comparison to the deforested area may be again explained by the incomplete combustion of the organic matter [74,77,78], forest floor decomposition [79], and leaching of partially pyrolyzed plant residues [14,71] and organic compounds in ash [77], due to the precipitation after the wildfire. Most studies state that OM content usually decreases in wildfire-affected areas, due to the combustion of plant biomass and organic soil layers [80,81]. Since OM and WSA are strongly associated, a decrease in OM can result in less stable aggregation of soil [63,65]. In contrast to what is above, some relevant studies support this explanation, since increased OM in burned areas has been recorded compared to the unburned sites after low to moderate fires (e.g., prescribed fires [77,82]). The significant decrease in WSA detected in the deforested soils could be again associated with the reduction in OM, and this agrees with the findings by refs. [83,84], who stated that soil aggregate stability follows the evolutionary dynamics of OM. Under this condition, the decrease in OM should be ascribed to the drastic removal of vegetation, which led to a high mineralisation of organic compounds (e.g., [85,86]). Theoretically, also the action of root systems in grasses may influence the OM stock in soil and noticeably impact its structure [87–89]. However, the dominance of herbaceous plants with root systems not well developed in the most superficial layer of topsoil suggested giving less emphasis to the actions of the morphological traits of roots on rill detachment capacity, which is a process acting only on the soil surface.

Concerning the rill erosion process, this investigation has shown that deforestation can significantly increase D_c (+35%) compared to fire with a low severity. The comparison of D_c measured in the burned and deforested soils of this investigation to the values reported in the parent study by ref. [52] for undisturbed soils shows that the wildfire increases D_c by 155% and deforestation by even 289%. Again, the increases in particle detachment in rills must be ascribed to the noticeable changes in the soil properties due to fire and, especially, deforestation [43,90–92]. Also, soil compaction due to heavy machinery on deforested sites might have affected both WSA and OM, and, indirectly, D_c. Compaction reduces soil porosity, limiting water infiltration and plant root penetration, therefore exacerbating soil's susceptibility to erosion and increasing the rill detachment capacity. Moreover, deforestation and soil compaction usually lead to important losses of soil organic carbon and reduction of WSA [93], thus leading to soil degradation [94].

4.2. Analysis of Correlations Between Soil Parameters and Discrimination Between Burned and Deforested Soils

The correlation analysis has shown close and inverse associations between the studied properties (OM and WSA) of soil, and its erodibility due to rill flow. These relationships explain why D_c significantly increases in burned and deforested sites. The scientific literature is quite unanimous about the decrease in D_c when soil OM (e.g., [95]) or aggregate stability (e.g., [96]) or both parameters (e.g., [19]) increase. Many other studiees have shown that the two soil properties adopted in this study as drivers of the rill detachment process have significant effects on D_c [97–99]. Therefore, these variables are key parameters for accurate estimations of D_c, and this implies that the studied soil properties have important effects on D_c and can be used for modelling purposes.

Another aspect that confirms the close associations among the three soil parameters measured in this study is the existence of one derivative variable (that is, the PC1) that is simultaneously and noticeably influenced by WSA, OM, and D_c (although with different effects). This variable can, therefore, be adopted as a measure of the effects of soil

disturbance due to fire or deforestation on the forest ecosystem, since it synthesises the variability of more properties between different soil conditions in one parameter.

An important result of this study is the noticeable, although not extreme, discrimination between the two soil conditions revealed by PCA and AHCA in a quantitative approach. This differentiation demonstrates that the effects of fire and deforestation are noticeably variable between the two soil conditions as the result of the different processes behind these forest disturbances (e.g., vegetation burning, soil heating, hydrophobicity, ash leaching—for burned sites—and tree cutting, logging, soil compaction—for deforestation—[13,17,100,101]).

4.3. Modelling Rill Detachment Capacity in Burned and Deforested Soils

Simple but accurate models to estimate the rill detachment capacity from some easily measurable parameters are of utmost importance for land managers and hydrologists. To this aim, several studies have proposed equations with different structures and input parameters (e.g., hydraulic and/or soil variables), to estimate D_c in a variety of environments and land conditions [96,102].

The evaluation of the effects of disturbances and land use changes on rill erodibility and critical shear stress is an important issue, since $K_{r\ c}$ is an essential parameter of soil resistance to runoff [19,25] and is a sensitive input variable in physically based erosion models [26,95,103], such as the WEPP model [104]. The linear equations that interpolate D_c and τ show high accuracy in predicting K_r for burned and deforested sites. These linear models reveal that not only is D_c higher in deforested sites compared to the burned areas, but K_r increases by about 5%. The K_r in both burned and deforested sites is more than 2.5-fold the value (0.0036 s m^{-1}) measured by [52] in undisturbed soils under the same environmental conditions. Also, ref. [105] estimated a high decrease in K_r on steep hillslopes throughout two years after a wildfire, and ref. [84] found a consistent result in burned pine stands compared to dense shrublands. All authors agree on the significant contribution of the changes in important soil properties to the increase in soil erodibility after a wildfire. However, other drivers of soil erosion (i.e., fire intensity, slope gradient, weather conditions) play a noticeable role in these factors of ecosystem degradation [106–108].

The high accuracy of the two equations proposed in this study to predict D_c is in close agreement with other studies. In this regard, ref. [102] found a very high accuracy of linear regressions between D_c and τ under different land uses in the Loess Plateau of China. The accuracy of models with the same structure set up by [43] in deforested and deforested sites of Northern Iran was highlighted by an r^2 in the range of 0.86–0.88. This accuracy was even higher in soils deforested and treated with rice husk biochar (r^2 = 0.89–0.93) [109] and with four different land uses (r^2 = 0.90–0.98, croplands, grasslands, forestlands, and woodlands, again in Northern Iran) [19].

Other mathematical forms (logarithmic, power, and exponential) in addition to linear expressions were checked in this study to interpolate the pairs D_c-τ. Only a power function (that is, $D_c = a\tau^b$, *a* and *b* being regression coefficients) gave higher interpolation accuracy (r^2 = 0.87 and 0.92 for deforested and burned soils, respectively) compared to a linear equation. However, according to [57] and other authors, a linear equation should still be preferred, since this allows the calculation of K_r, which is an essential parameter to be used as input in physically based models to predict erosion.

5. Conclusions

The comparison of key soil properties measured in deforested and burned sites in forestlands of Northern Iran has shown increases in the organic matter and aggregate stability by 15% and 34%, respectively, after deforestation compared to the wildfire-affected soils. Due to the close associations among WSA, OM, and D_c (shown by the correlation analysis), deforestation impacts soil erodibility more than fire (+35%). These unexpected results may be explained by the low severity of the fire, which moderately changed those

soil properties, and the use of heavy machinery for deforestation, which may have noticeably compacted the soil.

According to PCA and AHCA, wildfire and deforestation noticeably discriminate (although not sharply) burned from deforested sites, and therefore separate models must be set up to predict rill erosion for the two conditions.

The simulation of the rill detachment process by flume experiments gave accurate linear equations interpolating D_c and τ. These linear models allow the estimation of K_r (an essential parameter of soil resistance when using erosion models) under the two soil conditions. Clearly, the models proposed in this study are not original but were adapted to the need for prediction tools of rill detachment capacity in sites deforested and burned by high-severity fires (surprisingly little used for modelling soil hydrology). This adaptation has provided the rill erodibility under these soil disturbances. Therefore, these models may be used for erosion predictions in areas with similar climatic and geomorphological characteristics to the experimental sites (e.g., the burned and deforested areas in the Mediterranean basin). More research is needed to extrapolate the proposed models to different environmental contexts and under a variety of land and weather conditions for their ultimate validation.

Overall, this study provides insight into the hydrological effects of two severe disturbances (namely fire and deforestation) on soil erodibility, and simple tools for the predictions of key physical variables associated with the rill detachment process, in order to help land managers and hydrologists to limit the degradation rate and hydrological hazards in delicate forest ecosystems.

Author Contributions: Conceptualization, M.P., D.A.Z. and M.E.L.-B.; methodology, M.P., D.A.Z. and M.E.L.-B.; validation, M.P., D.A.Z. and M.E.L.-B.; formal analysis, M.P., D.A.Z. and M.E.L.-B.; investigation, M.P.; resources, D.A.Z.; data curation, M.P.; writing—original draft preparation, M.P.; writing—review and editing, M.P., D.A.Z. and M.E.L.-B.; supervision, D.A.Z. and M.E.L.-B.; project administration, D.A.Z.; funding acquisition, D.A.Z. All authors have read and agreed to the published version of the manuscript.

Funding: Partial financial support was received from the Faculty of Agricultural Sciences, University of Guilan, Iran.

Data Availability Statement: The datasets generated and analysed during the current study are available from the corresponding author upon reasonable request.

Conflicts of Interest: The authors declare no conflicts of interest.

Appendix A

Table A1. Soil detachment capacity, organic matter, and aggregate stability in water of soil collected in burned and deforested sites for flume experiments at given slope and water flow rates on soil samples in the study area (Khortum Forestland Park, Northern Iran).

Soil Slope (%)	Water Flow Rate (L s^{-1})	Soil Detachment Capacity (kg m^{-2} s^{-1})		Organic Matter (%)		Water Aggregate Stability (mm)	
		D	B	D	B	D	B
4.2	0.062	0.011	0.031	1.26	1.23	0.33	0.27
	0.084	0.015	0.039	1.25	1.22	0.32	0.24
	0.110	0.017	0.048	1.24	1.24	0.31	0.24
	0.134	0.021	0.059	1.35	1.11	0.29	0.25
	0.158	0.027	0.067	1.29	1.21	0.29	0.21
10.2	0.062	0.018	0.043	1.28	1.11	0.25	0.18
	0.084	0.023	0.051	1.26	1.18	0.28	0.18
	0.110	0.027	0.063	1.35	1.21	0.22	0.15
	0.134	0.039	0.071	1.22	1.11	0.21	0.18
	0.158	0.044	0.081	1.21	1.09	0.29	0.17

16.1	0.062	0.026	0.061	1.24	1.02	0.25	0.15
	0.084	0.047	0.074	1.21	1.07	0.29	0.18
	0.110	0.053	0.081	1.33	0.95	0.28	0.28
	0.134	0.069	0.089	1.23	0.91	0.21	0.27
	0.158	0.078	0.091	1.19	0.91	0.25	0.26
24.4	0.062	0.041	0.076	1.26	1.11	0.24	0.18
	0.084	0.054	0.089	1.19	1.12	0.26	0.15
	0.110	0.073	0.097	1.31	1.09	0.21	0.16
	0.134	0.089	0.176	1.18	0.89	0.27	0.13
	0.158	0.139	0.192	1.19	0.86	0.16	0.13
33.6	0.062	0.059	0.089	1.06	1.14	0.33	0.13
	0.084	0.077	0.098	1.11	1.09	0.22	0.17
	0.110	0.139	0.182	1.01	0.87	0.19	0.14
	0.134	0.155	0.189	1.05	0.82	0.16	0.16
	0.158	0.186	0.198	1.02	0.81	0.17	0.14

Note: D = deforested soil; B = burned soil.

References

1. Kelly, L.T.; Giljohann, K.M.; Duane, A.; Aquilué, N.; Archibald, S.; Batllori, E.; Bennett, A.F.; Buckland, S.T.; Canelles, Q.; Clarke, M.F.; et al. Fire and Biodiversity in the Anthropocene. *Science* **2020**, *370*, eabb0355. https://doi.org/10.1126/science.abb0355.
2. Babur, E.; Uslu, Ö.S.; Battaglia, M.L.; Diatta, A.; Fahad, S.; Datta, R.; Zafar-ul-Hye, M.; Hussain, G.S.; Danish, S. Studying Soil Erosion by Evaluating Changes in Physico-Chemical Properties of Soils under Different Land-Use Types. *J. Saudi Soc. Agric. Sci.* **2021**, *20*, 190–197.
3. Braun, A.C. Deforestation by Afforestation: Land Use Change in the Coastal Range of Chile. *Remote Sens.* **2022**, *14*, 1686.
4. Wu, S.; Li, D.; Liu, L.; Zhang, W.; Liu, K.; Zhao, W.; Shen, J.; Hao, C.; Zhang, L. Global Patterns and Influencing Factors of Post-Fire Land Cover Change. *Glob. Planet. Chang.* **2023**, *223*, 104076.
5. Karamage, F.; Shao, H.; Chen, X.; Ndayisaba, F.; Nahayo, L.; Kayiranga, A.; Omifolaji, J.K.; Liu, T.; Zhang, C. Deforestation Effects on Soil Erosion in the Lake Kivu Basin, DR Congo-Rwanda. *Forests* **2016**, *7*, 281.
6. Neris, J.; Robichaud, P.R.; Wagenbrenner, J.W.; Brown, R.E.; Doerr, S.H. Soil Erosion after Fire in Volcanic Terrain: Assessment and Implications for Post-Fire Soil Losses. *J. Hydrol.* **2023**, *625*, 129923.
7. Lindner, M.; Maroschek, M.; Netherer, S.; Kremer, A.; Barbati, A.; Garcia-Gonzalo, J.; Seidl, R.; Delzon, S.; Corona, P.; Kolström, M. Climate Change Impacts, Adaptive Capacity, and Vulnerability of European Forest Ecosystems. *For. Ecol. Manag.* **2010**, *259*, 698–709.
8. Raiesi, F.; Beheshti, A. Evaluating Forest Soil Quality after Deforestation and Loss of Ecosystem Services Using Network Analysis and Factor Analysis Techniques. *Catena* **2022**, *208*, 105778.
9. Vereecken, H.; Schnepf, A.; Hopmans, J.W.; Javaux, M.; Or, D.; Roose, T.; Vanderborght, J.; Young, M.H.; Amelung, W.; Aitkenhead, M. Modeling Soil Processes: Review, Key Challenges, and New Perspectives. *Vadose Zone J.* **2016**, *15*, 1–57. https://doi.org/10.2136/vzj2015.09.0131.
10. Dragović, N.; Vulević, T. Soil Degradation Processes, Causes, and Assessment Approaches. In *Life on Land*; Springer: Berlin/Heidelberg, Germany, 2020; pp. 928–939.
11. García-Ruiz, J.M.; Nadal-Romero, E.; Lana-Renault, N.; Beguería, S. Erosion in Mediterranean Landscapes: Changes and Future Challenges. *Geomorphology* **2013**, *198*, 20–36.
12. Moody, J.A.; Martin, D.A. Initial Hydrologic and Geomorphic Response Following a Wildfire in the Colorado Front Range. *Earth Surf. Process. Landf. J. Br. Geomorphol. Res. Group* **2001**, *26*, 1049–1070.
13. Shakesby, R.A. Post-Wildfire Soil Erosion in the Mediterranean: Review and Future Research Directions. *Earth Sci. Rev.* **2011**, *105*, 71–100.
14. Agbeshie, A.A.; Abugre, S.; Atta-Darkwa, T.; Awuah, R. A Review of the Effects of Forest Fire on Soil Properties. *J. For. Res.* **2022**, *33*, 1419–1441.
15. Zavala, L.M.M.; de Celis Silvia, R.; López, A.J. How Wildfires Affect Soil Properties. A Brief Review. *Cuad. Investig. Geogr. Geogr. Res. Lett.* **2014**, *40*, 311–331.
16. Bodí, M.B.; Cerdà, A.; Mataix-Solera, J.; Doerr, S.H. A Review of Fire Effects on Vegetation and Soil in the Mediterranean Basin. *Bol. Asoc. Geógr. Esp.* **2012**, 439–441.
17. Moody, J.A.; Shakesby, R.A.; Robichaud, P.R.; Cannon, S.H.; Martin, D.A. Current Research Issues Related to Post-Wildfire Runoff and Erosion Processes. *Earth Sci. Rev.* **2013**, *122*, 10–37.
18. Restrepo, J.D.; Kettner, A.J.; Syvitski, J.P. Recent Deforestation Causes Rapid Increase in River Sediment Load in the Colombian Andes. *Anthropocene* **2015**, *10*, 13–28.

19. Parhizkar, M.; Shabanpour, M.; Khaledian, M.; Cerdà, A.; Rose, C.W.; Asadi, H.; Lucas-Borja, M.E.; Zema, D.A. Assessing and Modeling Soil Detachment Capacity by Overland Flow in Forest and Woodland of Northern Iran. *Forests* **2020**, *11*, 65.
20. Zhang, G.-H.; Liu, B.-Y.; Nearing, M.A.; Huang, C.-H.; Zhang, K.-L. Soil Detachment by Shallow Flow. *Trans. ASAE* **2002**, *45*, 351.
21. Foster, G.R.; Meyer, L.D. Transport of Soil Particles by Shallow Flow. *Trans. ASAE* **1972**, *15*, 99–0102.
22. Nearing, M.A.; Bradford, J.M.; Parker, S.C. Soil Detachment by Shallow Flow at Low Slopes. *Soil Sci. Soc. Am. J.* **1991**, *55*, 339–344.
23. Li, D.; Chen, X.; Han, Z.; Gu, X.; Li, Y. Determination of Rill Erodibility and Critical Shear Stress of Saturated Purple Soil Slopes. *Int. Soil Water Conserv. Res.* **2022**, *10*, 38–45.
24. Lee, S.; Chu, M.L.; Guzman, J.A.; Flanagan, D.C. Modeling Soil Erodibility and Critical Shear Stress Parameters for Soil Loss Estimation. *Soil Tillage Res.* **2022**, *218*, 105292.
25. Nearing, M.A.; Foster, G.R.; Lane, L.J.; Finkner, S.C. A Process-Based Soil Erosion Model for USDA-Water Erosion Prediction Project Technology. *Trans. ASAE* **1989**, *32*, 1587–1593.
26. Wang, D.; Wang, Z.; Shen, N.; Chen, H. Modeling Soil Detachment Capacity by Rill Flow Using Hydraulic Parameters. *J. Hydrol.* **2016**, *535*, 473–479.
27. McGuire, L.A.; Pelletier, J.D.; Gómez, J.A.; Nearing, M.A. Controls on the Spacing and Geometry of Rill Networks on Hillslopes: Rain Splash Detachment, Initial Hillslope Roughness, and the Competition between Fluvial and Colluvial Transport. *J. Geophys. Res. Earth Surf.* **2013**, *118*, 241–256.
28. Polyakov, V.O.; Nearing, M.A. Sediment Transport in Rill Flow under Deposition and Detachment Conditions. *Catena* **2003**, *51*, 33–43.
29. Knapen, A.; Poesen, J.; Govers, G.; Gyssels, G.; Nachtergaele, J. Resistance of Soils to Concentrated Flow Erosion: A Review. *Earth-Sci. Rev.* **2007**, *80*, 75–109.
30. Wang, H.; Zhang, G. Temporal Variation in Soil Erodibility Indices for Five Typical Land Use Types on the Loess Plateau of China. *Geoderma* **2021**, *381*, 114695.
31. Aksoy, H.; Kavvas, M.L. A Review of Hillslope and Watershed Scale Erosion and Sediment Transport Models. *Catena* **2005**, *64*, 247–271.
32. Filianoti, P.; Gurnari, L.; Zema, D.A.; Bombino, G.; Sinagra, M.; Tucciarelli, T. An Evaluation Matrix to Compare Computer Hydrological Models for Flood Predictions. *Hydrology* **2020**, *7*, 42.
33. Fernández, C.; Vega, J.A. Evaluation of the Rusle and Disturbed Wepp Erosion Models for Predicting Soil Loss in the First Year after Wildfire in NW Spain. *Environ. Res.* **2018**, *165*, 279–285. https://doi.org/10.1016/j.envres.2018.04.008.
34. Lucas-Borja, M.E.; Plaza-Alvarez, P.A.; Xu, X.; Carra, B.G.; Zema, D.A. Exploring the Factors Influencing the Hydrological Response of Soil after Low and High-Severity Fires with Post-Fire Mulching in Mediterranean Forests. *Int. Soil Water Conserv. Res.* **2022**, *11*, 169–182.
35. Mataix-Solera, J.; Gómez, I.; Navarro-Pedreño, J.; Guerrero, C.; Moral, R. Soil Organic Matter and Aggregates Affected by Wildfire in a Pinus Halepensis Forest in a Mediterranean Environment. *Int. J. Wildland Fire* **2002**, *11*, 107–114. https://doi.org/10.1071/wf02020.
36. Khormali, F.; Ajami, M.; Ayoubi, S.; Srinivasarao, C.; Wani, S.P. Role of Deforestation and Hillslope Position on Soil Quality Attributes of Loess-Derived Soils in Golestan Province, Iran. *Agric. Ecosyst. Environ.* **2009**, *134*, 178–189.
37. Efthimiou, N.; Psomiadis, E.; Panagos, P. Fire Severity and Soil Erosion Susceptibility Mapping Using Multi-Temporal Earth Observation Data: The Case of Mati Fatal Wildfire in Eastern Attica, Greece. *Catena* **2020**, *187*, 104320.
38. Evelpidou, N.; Tzouxanioti, M.; Gavalas, T.; Spyrou, E.; Saitis, G.; Petropoulos, A.; Karkani, A. Assessment of Fire Effects on Surface Runoff Erosion Susceptibility: The Case of the Summer 2021 Forest Fires in Greece. *Land* **2021**, *11*, 21.
39. Riquetti, N.B.; Beskow, S.; Guo, L.; Mello, C.R. Soil Erosion Assessment in the Amazon Basin in the Last 60 Years of Deforestation. *Environ. Res.* **2023**, *236*, 116846.
40. Camarasa-Belmonte, A.M.; Rubio, M.; Salas, J. Rainfall Events and Climate Change in Mediterranean Environments: An Alarming Shift from Resource to Risk in Eastern Spain. *Nat. Hazards* **2020**, *103*, 423–445.
41. Change, I.C. Land: An IPCC Special Report on Climate Change, Desertification, Land Degradation, Sustainable Land Management, Food Security, and Greenhouse Gas Fluxes in Terrestrial Ecosystems. Summary for Policymakers. 2019. Available online: https://www.ipcc.ch/srccl/ (accessed on 20 July 2024).
42. Fernández, C.; Vega, J.A. Are Erosion Barriers and Straw Mulching Effective for Controlling Soil Erosion after a High Severity Wildfire in NW Spain? *Ecol. Eng.* **2016**, *87*, 132–138. https://doi.org/10.1016/j.ecoleng.2015.11.047.
43. Parhizkar, M.; Shabanpour, M.; Zema, D.A.; Lucas-Borja, M.E. Rill Erosion and Soil Quality in Forest and Deforested Ecosystems with Different Morphological Characteristics. *Resources* **2020**, *9*, 129. https://doi.org/10.3390/resources9110129.
44. Gholoubi, A.; Emami, H.; Alizadeh, A.; Azadi, R. Long Term Effects of Deforestation on Soil Attributes: Case Study, Northern Iran. *Casp. J. Environ. Sci.* **2019**, *17*, 73–81.
45. Fernández, C.; Fernández-Alonso, J.M.; Vega, J.A. Exploring the Effect of Hydrological Connectivity and Soil Burn Severity on Sediment Yield after Wildfire and Mulching. *Land Degrad. Dev.* **2020**, *31*, 1611–1621.
46. Shabanpour, M.; Daneshyar, M.; Parhizkar, M.; Lucas-Borja, M.E.; Antonio Zema, D. Influence of Crops on Soil Properties in Agricultural Lands of Northern Iran. *Sci. Total Environ.* **2020**, *711*, 134694. https://doi.org/10.1016/j.scitotenv.2019.134694.

47. Zhou, C.; Shen, N.; Zhang, F.; Delang, C.O. Soil Detachment by Sediment-Laden Rill Flow Interpreted Using Three Experimental Design Methods. *Catena* **2022**, *215*, 106332.
48. Ma, J.; Li, Z.; Sun, B.; Ma, B.; Zhang, L. Modeling Soil Detachment Capacity by Rill Flow under the Effect of Freeze–Thaw and the Root System. *Nat. Hazards* **2022**, *112*, 207–230. https://doi.org/10.1007/s11069-021-05178-7.
49. Kottek, M.; Grieser, J.; Beck, C.; Rudolf, B.; Rubel, F. World Map of the Köppen-Geiger Climate Classification Updated. *Meteorol. Z.* **2006**, *15*, 259–263.
50. Sedaghatkish, F.; Asadi Kapourchal, S.; Parhizkar, M. Oriental Beech Roots Improve Soil Aggregate Stability and Reduce Soil Detachment Rate in Forest Lands. *Rhizosphere* **2023**, *27*, 100744. https://doi.org/10.1016/j.rhisph.2023.100744.
51. Fornwalt, P.J.; Kaufmann, M.R.; Stohlgren, T.J. Impacts of Mixed Severity Wildfire on Exotic Plants in a Colorado Ponderosa Pine–Douglas-Fir Forest. *Biol. Invasions* **2010**, *12*, 2683–2695.
52. Parhizkar, M.; Cerdà, A. Modelling Effects of Human-Caused Fires on Rill Detachment Capacity Based on Surface Burning of Soils in Forest Lands. *J. Hydrol.* **2023**, *624*, 129893.
53. Ryan, K.C. Dynamic Interactions between Forest Structure and Fire Behavior in Boreal Ecosystems. *Silva Fenn.* **2002**, *36*, 13–39.
54. Shanshan, W.; Baoyang, S.; Chaodong, L.; Zhanbin, L.; Bo, M. Runoff and soil erosion on slope Cropland: A Review. *J. Resour. Ecol.* **2018**, *9*, 461–470.
55. Ghasemzadeh, Z.; Parhizkar, M.; Mirmohammadmeygooni, S.; Shabanpour, M.; Chalmers, G. Forest Soil Inoculation with Bacillus Subtilus Reduces Soil Detachment Rate to Mitigate Rill Erosion. *Rhizosphere* **2023**, *26*, 100707. https://doi.org/10.1016/j.rhisph.2023.100707.
56. Shen, N.; Wang, Z.; Guo, Q.; Zhang, Q.; Wu, B.; Liu, J.; Ma, C.; Delang, C.O.; Zhang, F. Soil Detachment Capacity by Rill Flow for Five Typical Loess Soils on the Loess Plateau of China. *Soil Tillage Res.* **2021**, *213*, 105159. https://doi.org/10.1016/j.still.2021.105159.
57. Ou, X.; Hu, Y.; Li, X.; Guo, S.; Liu, B. Advancements and challenges in rill formation, morphology, measurement and modeling. *Catena* **2021**, *196*, 104932.
58. Di Stefano, C.; Ferro, V.; Palmeri, V.; Pampalone, V. Flow Resistance Equation for Rills. *Hydrol. Process.* **2017**, *31*, 2793–2801.
59. Luk, S.H.; Merz, W. Use of the Salt Tracing Technique to Determine the Velocity of Overland Flow. *Soil Technol.* **1992**, *5*, 289–301.
60. Ma, Q.; Zhang, K.; Cao, Z.; Yang, Z.; Wei, M.; Gu, Z. Impacts of Different Surface Features on Soil Detachment in the Subtropical Region. *Int. Soil Water Conserv. Res.* **2021**, *9*, 555–565.
61. Abrahams, A.D.; Parsons, A.J.; Luk, S.-H. Field Measurement of the Velocity of Overland Flow Using Dye Tracing. *Earth Surf. Process. Landf.* **1986**, *11*, 653–657.
62. Schäffer, B.; Stauber, M.; Müller, R.; Schulin, R. Changes in the Macro-pore Structure of Restored Soil Caused by Compaction beneath Heavy Agricultural Machinery: A Morphometric Study. *Eur. J. Soil Sci.* **2007**, *58*, 1062–1073.
63. Parhizkar, M.; Lucas-Borja, M.E.; Zema, D.A. Changes in Rill Detachment Capacity after Deforestation and Soil Conservation Practices in Forestlands of Northern Iran. *Catena* **2024**, *246*, 108405.
64. Baldassini, P.; Paruelo, J.M. Deforestation and Current Management Practices Reduce Soil Organic Carbon in the Semi-Arid Chaco, Argentina. *Agric. Syst.* **2020**, *178*, 102749.
65. Mataix-Solera, J.; Cerdà, A.; Arcenegui, V.; Jordán, A.; Zavala, L.M. Fire Effects on Soil Aggregation: A Review. *Earth-Sci. Rev.* **2011**, *109*, 44–60.
66. Allison, L.E. Organic Carbon. In *Methods of Soil Analysis: Part 2*; American Society of Agronomy: Madison, WI, USA, 1965; pp. 1367–1376.
67. Kemper, W.D.; Rosenau, R.C. Aggregate Stability and Size Distribution. In *Methods of Soil Analysis: Part 1*; American Society of Agronomy: Madison, WI, USA, 1986; pp. 425–442.
68. Yamaguchi, A.; Kanashiki, N.; Ishizaki, H.; Kobayashi, M.; Osawa, K. Relationship between Soil Erodibility by Concentrated Flow and Shear Strength of a Haplic Acrisol with a Cationic Polyelectrolyte. *Catena* **2022**, *217*, 106506.
69. Lee Rodgers, J.; Nicewander, W.A. Thirteen Ways to Look at the Correlation Coefficient. *Am. Stat.* **1988**, *42*, 59–66.
70. Wade, C.M.; Austin, K.G.; Cajka, J.; Lapidus, D.; Everett, K.H.; Galperin, D.; Maynard, R.; Sobel, A. What Is Threatening Forests in Protected Areas? A Global Assessment of Deforestation in Protected Areas, 2001–2018. *Forests* **2020**, *11*, 539.
71. Caon, L.; Vallejo, V.R.; Ritsema, C.J.; Geissen, V. Effects of Wildfire on Soil Nutrients in Mediterranean Ecosystems. *Earth-Sci. Rev.* **2014**, *139*, 47–58.
72. Certini, G. Effects of Fire on Properties of Forest Soils: A Review. *Oecologia* **2005**, *143*, 1–10.
73. Alcañiz, M.; Úbeda, X.; Cerdà, A. A 13-Year Approach to Understand the Effect of Prescribed Fires and Livestock Grazing on Soil Chemical Properties in Tivissa, NE Iberian Peninsula. *Forests* **2020**, *11*, 1013. https://doi.org/10.3390/f11091013.
74. Úbeda, X.; Lorca, M.; Outeiro, L.R.; Bernia, S.; Castellnou, M. Effects of Prescribed Fire on Soil Quality in Mediterranean Grassland (Prades Mountains, North-East Spain). *Int. J. Wildland Fire* **2005**, *14*, 379. https://doi.org/10.1071/WF05040.
75. Varela, M.E.; Benito, E.; Keizer, J.J. Effects of Wildfire and Laboratory Heating on Soil Aggregate Stability of Pine Forests in Galicia: The Role of Lithology, Soil Organic Matter Content and Water Repellency. *CATENA* **2010**, *83*, 127–134.
76. Shakesby, R.A.; Doerr, S.H. Wildfire as a Hydrological and Geomorphological Agent. *Earth Sci. Rev.* **2006**, *74*, 269–307.
77. Alcañiz, M.; Outeiro, L.; Francos, M.; Úbeda, X. Effects of Prescribed Fires on Soil Properties: A Review. *Sci. Total Environ.* **2018**, *613*, 944–957.
78. Soto, B.; Diaz-Fierros, F. Interactions between Plant Ash Leachates and Soil. *Int. J. Wildland Fire* **1993**, *3*, 207–216.

79. Scharenbroch, B.C.; Nix, B.; Jacobs, K.A.; Bowles, M.L. Two Decades of Low-Severity Prescribed Fire Increases Soil Nutrient Availability in a Midwestern, USA Oak (Quercus) Forest. *Geoderma* **2012**, *183*, 80–91.
80. Pellegrini, A.F.; Harden, J.; Georgiou, K.; Hemes, K.S.; Malhotra, A.; Nolan, C.J.; Jackson, R.B. Fire Effects on the Persistence of Soil Organic Matter and Long-Term Carbon Storage. *Nat. Geosci.* **2022**, *15*, 5–13.
81. Lucas-Borja, M.E.; Ortega, R.; Miralles, I.; Plaza-Álvarez, P.A.; González-Romero, J.; Peña-Molina, E.; Moya, D.; Zema, D.A.; Wagenbrenner, J.W.; De las Heras, J. Effects of Wildfire and Logging on Soil Functionality in the Short-Term in Pinus Halepensis M. Forests. *Eur. J. For. Res.* **2020**, *139*, 935–945.
82. Lucas-Borja, M.E.; de las Heras, J.; Moya Navarro, D.; González-Romero, J.; Peña-Molina, E.; Navidi, M.; Fajardo-Cantos, Á.; Miralles Mellado, I.; Plaza-Alvarez, P.A.; Gianmarco Carrà, B.; et al. Short-Term Effects of Prescribed Fires with Different Severity on Rainsplash Erosion and Physico-Chemical Properties of Surface Soil in Mediterranean Forests. *J. Environ. Manag.* **2022**, *322*, 116143. https://doi.org/10.1016/j.jenvman.2022.116143.
83. Cerdà, A.; Imeson, A.C.; Calvo, A. Fire and Aspect Induced Differences on the Erodibility and Hydrology of Soils at La Costera, Valencia, Southeast Spain. *CATENA* **1995**, *24*, 289–304.
84. Giovannini, G.; Vallejo, R.; Lucchesi, S.; Bautista, S.; Ciompi, S.; Llovet, J. Effects of Land Use and Eventual Fire on Soil Erodibility in Dry Mediterranean Conditions. *For. Ecol. Manag.* **2001**, *147*, 15–23.
85. Kooch, Y.; Amani, M.; Abedi, M. The Effect of Shrublands Degradation Intensity on Soil Organic Matter-Associated Properties in a Semi-Arid Ecosystem. *Sci. Total Environ.* **2022**, *853*, 158664.
86. de Souza Medeiros, A.; Gonzaga, G.B.M.; da Silva, T.S.; de Souza Barreto, B.; dos Santos, T.C.; de Melo, P.L.A.; de Araújo Gomes, T.C.; Maia, S.M.F. Changes in Soil Organic Carbon and Soil Aggregation Due to Deforestation for Smallholder Management in the Brazilian Semi-Arid Region. *Geoderma Reg.* **2023**, *33*, e00647.
87. Baets, S.D.; Poesen, J.; Knapen, A.; Galindo, P. Impact of Root Architecture on the Erosion-reducing Potential of Roots during Concentrated Flow. *Earth Surf. Process. Landf. J. Br. Geomorphol. Res. Group* **2007**, *32*, 1323–1345.
88. Demenois, J.; Carriconde, F.; Bonaventure, P.; Maeght, J.-L.; Stokes, A.; Rey, F. Impact of Plant Root Functional Traits and Associated Mycorrhizas on the Aggregate Stability of a Tropical Ferralsol. *Geoderma* **2018**, *312*, 6–16.
89. Burak, E.; Dodd, I.C.; Quinton, J.N. A Mesocosm-based Assessment of Whether Root Hairs Affect Soil Erosion by Simulated Rainfall. *Eur. J. Soil Sci.* **2021**, *72*, 2372–2380.
90. de Dios Benavides-Solorio, J.; MacDonald, L.H. Measurement and Prediction of Post-Fire Erosion at the Hillslope Scale, Colorado Front Range. *Int. J. Wildland Fire* **2005**, *14*, 457–474.
91. Johansen, M.P.; Hakonson, T.E.; Breshears, D.D. Post-fire Runoff and Erosion from Rainfall Simulation: Contrasting Forests with Shrublands and Grasslands. *Hydrol. Process.* **2001**, *15*, 2953–2965.
92. Martin, D.A.; Moody, J.A. Comparison of Soil Infiltration Rates in Burned and Unburned Mountainous Watersheds. *Hydrol. Process.* **2001**, *15*, 2893–2903.
93. Mgelwa, A.S.; Ngaba, M.J.Y.; Hu, B.; Gurmesa, G.A.; Mwakaje, A.G.; Nyemeck, M.P.B.; Zhu, F.; Qiu, Q.; Song, L.; Wang, Y. Meta-Analysis of 21st Century Studies Shows That Deforestation Induces Profound Changes in Soil Characteristics, Particularly Soil Organic Carbon Accumulation. *For. Ecosyst.* **2024**, 100257.
94. Merino, A.; Omil, B.; Piñeiro, V.; Barros, N.; Souza-Alonso, P.; Campo, J. Soil C Dynamics after Deforestation and Subsequent Conversion of Arable Cropland to Grassland in Humid Temperate Areas. *Sci. Total Environ.* **2023**, *901*, 165793.
95. Knapen, A.; Poesen, J.; Govers, G.; De Baets, S. The Effect of Conservation Tillage on Runoff Erosivity and Soil Erodibility during Concentrated Flow. *Hydrol. Process. Int. J.* **2008**, *22*, 1497–1508.
96. Ciampalini, R.; Torri, D. Detachment of Soil Particles by Shallow Flow: Sampling Methodology and Observations. *Catena* **1998**, *32*, 37–53.
97. Govers, G.; Giménez, R.; Van Oost, K. Rill Erosion: Exploring the Relationship between Experiments, Modelling and Field Observations. *Earth-Sci. Rev.* **2007**, *84*, 87–102.
98. Pierson, F.B.; Moffet, C.A.; Williams, C.J.; Hardegree, S.P.; Clark, P.E. Prescribed-Fire Effects on Rill and Interrill Runoff and Erosion in a Mountainous Sagebrush Landscape. *Earth Surf. Process. Landf.* **2009**, *34*, 193–203. https://doi.org/10.1002/esp.1703.
99. Li, T.; Yu, P.; Liu, D.; Fu, Q.; Hou, R.; Zhao, H.; Xu, S.; Zuo, Y.; Xue, P. Effects of Biochar on Sediment Transport and Rill Erosion after Two Consecutive Years of Seasonal Freezing and Thawing. *Sustainability* **2021**, *13*, 6984.
100. DeBano, L.F. *Water Repellent Soils: A State-of-the-Art*; US Department of Agriculture, Forest Service, Pacific Southwest Forest and Range Experiment Station: Berkeley, CA, USA, 1981; Volume 46.
101. Shakesby, R.A. Fire as a Geomorphological Agent. In *Oxford Companion to the Earth*; Oxford University Press: Oxford, UK, 2000; pp. 347–348.
102. Zhang, G.-H.; Liu, G.-B.; Tang, K.-M.; Zhang, X.-C. Flow Detachment of Soils under Different Land Uses in the Loess Plateau of China. *Trans. ASABE* **2008**, *51*, 883–890.
103. Geng, R.; Zhang, G.; Ma, Q.; Wang, L. Soil Resistance to Runoff on Steep Croplands in Eastern China. *Catena* **2017**, *152*, 18–28.
104. Laflen, J.M.; Lane, L.J.; Foster, G.R. WEPP: A New Generation of Erosion Prediction Technology. *J. Soil Water Conserv.* **1991**, *46*, 34–38.
105. Sheridan, G.J.; Noske, P.J.; Lane, P.N.; Sherwin, C.B. Using Rainfall Simulation and Site Measurements to Predict Annual Interrill Erodibility and Phosphorus Generation Rates from Unsealed Forest Roads: Validation against in-Situ Erosion Measurements. *Catena* **2008**, *73*, 49–62.

106. Hrelja, I.; Šestak, I.; Bogunović, I. Wildfire Impacts on Soil Physical and Chemical Properties-a Short Review of Recent Studies. *Agric. Conspec. Sci.* **2020**, *85*, 293–301.
107. Peduto, D.; Iervolino, L.; Foresta, V. Experimental Analysis of the Fire-Induced Effects on the Physical, Mechanical, and Hydraulic Properties of Sloping Pyroclastic Soils. *Geosciences* **2022**, *12*, 198.
108. Terefe, T.; Mariscal-Sancho, I.; Peregrina, F.; Espejo, R. Influence of Heating on Various Properties of Six Mediterranean Soils. A Laboratory Study. *Geoderma* **2008**, *143*, 273–280.
109. Parhizkar, M.; Shabanpour, M.; Lucas-Borja, M.E.; Zema, D.A. Effects of Rice Husk Biochar on Rill Detachment Capacity in Deforested Hillslopes. *Ecol. Eng.* **2023**, *191*, 106964. https://doi.org/10.1016/j.ecoleng.2023.106964.